

Tunneling into the Mott insulator Sr₂IrO₄

John Nichols,¹ Noah Bray-Ali,^{2,3} Armin Ansary,¹ Gang Cao,¹ and Kwok-Wai Ng¹

¹Center for Advanced Materials, Department of Physics and Astronomy, University of Kentucky, Lexington, Kentucky 40506-0055, USA

²Joint Quantum Institute, University of Maryland, College Park, Maryland 20742-4111, USA

³National Institute of Standards and Technology, Gaithersburg, Maryland 20899, USA

(Received 22 August 2012; revised manuscript received 13 December 2013; published 24 February 2014)

We studied the single-layered iridate Sr₂IrO₄ with a scanning tunneling microscope. The finite low temperature conductance enables the electronic structure of this antiferromagnetic Mott insulator to be measured by tunneling spectroscopy. We imaged the topography of freshly cleaved surfaces and measured differential tunneling conductance at cryogenic temperatures. We found the Mott gap in the tunneling density of states to be $2\Delta = 615$ meV. Within the Mott gap, additional shoulders are observed which are interpreted as inelastic loss features due to magnons.

DOI: [10.1103/PhysRevB.89.085125](https://doi.org/10.1103/PhysRevB.89.085125)

PACS number(s): 73.23.Hk, 71.70.Ej, 71.27.+a, 71.30.+h

I. INTRODUCTION

Recently, there has been a surge of renewed interest in $5d$ transition metal oxides, such as the iridates. The electrons in these compounds are more spatially extended than in their $3d$ and $4d$ counterparts, resulting in a smaller Coulomb interaction (U) and a larger bandwidth (W). This should make $5d$ transition-metal oxides metallic; however, it is believed that the large spin-orbit coupling (SOC) in the $5d$ materials drives some of them insulating. The prototype of this spin-orbit-driven insulating behavior is the single-layered iridate Sr₂IrO₄.

Tunneling spectroscopy is the most direct method for probing a material's density of states. It is a single particle probe capable of measuring both occupied and unoccupied states. This is of particular interest for Mott insulators since their density of states is not well understood and often has contributions from multiple excitations. Sr₂IrO₄ has been experimentally shown to be insulating for temperatures up to 600 K [1], due to the SOC parameter being large enough to allow the modest Coulomb interaction present in this material to open a Mott gap. The insulating gap has been previously estimated by angle resolved photoemission spectroscopy [2] (ARPES), optical conductivity [3], and resonant inelastic x-ray spectroscopy [4] (RIXS) which have the limitations of only being able to probe occupied states, being a two-particle probe, and limited energy resolution, respectively. Thus, we use scanning tunneling spectroscopy (STS) to directly measure the Mott gap in this material. Since tunneling spectroscopy is mostly sensitive to the charge property of electrons, magnon excitations are rarely seen in tunneling experiments [5–7]. Interestingly, in the present study, the SOC in Sr₂IrO₄ allows an anomalous magnon feature to be seen, which has also been measured in RIXS [4], Raman spectroscopy [8], and infrared spectroscopy [9]. Although we are the first group to investigate Sr₂IrO₄ with tunneling spectroscopy, there have been subsequent studies [10,11].

Sr₂IrO₄ has a tetragonal K₂NiF₄-like crystal structure as illustrated in Figs. 1(a) and 1(b). The lattice parameters of this material are $a = 5.499$ Å and $c = 25.799$ Å [12]. The IrO₆ octahedra undergo a rotation about the c axis of approximately 11° resulting in a reduced tetragonal crystal structure (space group I4₁/acd). The Ir atoms form a fourfold symmetric layer with a nearest neighbor separation of $a/\sqrt{2} = 3.888$ Å.

This material has five valence electrons to fill the $5d$ orbital. Crystal fields split this band into a lower-energy t_{2g} band and a higher-energy e_g band. SOC then splits the t_{2g} band into the $J_{\text{eff},3/2}$ state that is filled with four electrons, and the more highly energetic $J_{\text{eff},1/2}$ state is half filled with the remaining electron. The effects of band splitting due to crystal fields and SOC are shown in Fig. 1(c). The modest Coulomb interaction in the $J_{\text{eff},1/2}$ band forces this material into an insulating state [13] as shown in Fig. 1(d).

Below the Néel temperature ($T_N = 240$ K), canted antiferromagnetic order arises in the $J_{\text{eff},1/2}$ Ir moments of Sr₂IrO₄ [14,15]. The rotation of the IrO₆ octahedra and the staggered moment of $|\vec{S}_0| = 0.307$ [16] leads to a bulk ferromagnetic moment of $0.14 \mu_B$ per Ir ion [15]. It has also been reported that this material has additional magnetic ordering below T_N with transition temperatures of ~ 100 K and ~ 25 K measured by bulk magnetometry and muon studies [17].

Remarkably, even though Sr₂IrO₄ has an insulating ground state, it maintains a finite, nonzero electrical conductance even at cryogenic temperatures [1], uniquely allowing tunneling measurements to be performed. Similar tunneling experiments have been successfully performed on other Mott-insulating, transition-metal-oxide systems such as Ca₃Ru₂O₇ [18] and Ca₂CuO₂Cl₂ [19]. In this review, we report measurements of the atomic-scale lattice structure and electronic structure of single crystalline Sr₂IrO₄ using a scanning tunneling microscope (STM).

II. RESULTS

Tunneling measurements were conducted with a low-temperature STM [20]. The STM was oriented vertically inside a cryogenic probe, allowing for *in situ* sample cleaving and exchange. High quality single crystals of Sr₂IrO₄ were oriented such that the c axis was parallel to the STM tip. The samples were cleaved *in situ* by breaking off a small rod that was attached to the top of the sample.

An atomically resolved topographic image of the sample surface is presented in Fig. 2 and was acquired using an electrochemically etched tungsten tip. The image was obtained with a constant tunneling current of $I_{\text{set}} = 600$ pA at a sample bias voltage of $V_{\text{bias}} = 450$ mV. A square grid of atoms is visible with an atomic spacing of about 4.0 Å which is

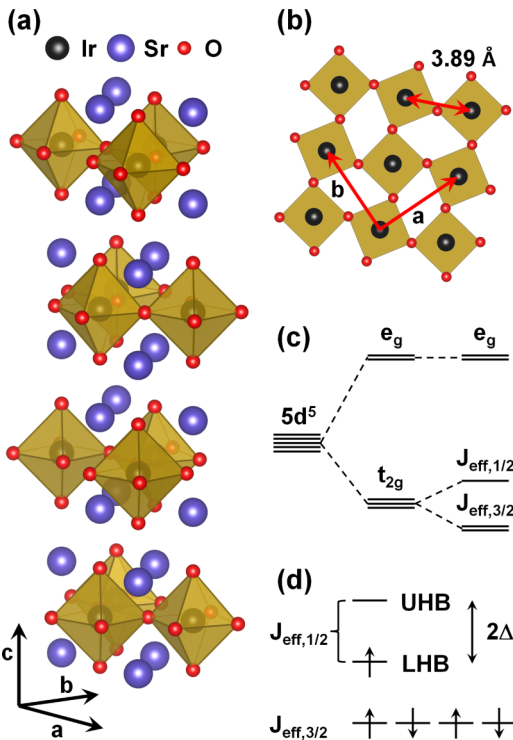


FIG. 1. (Color online) Crystal structure of Sr_2IrO_4 with a projection along (a) an arbitrary direction and (b) the c axis, where the Ir, Sr, and O atoms are black, blue, and red, respectively. The IrO_6 octahedra are colored dark yellow. (c) Illustration of how the $5d$ orbital is split due to crystal field splitting and spin-orbit coupling. (d) Illustration of the effect of the Coulomb interaction on the $J_{\text{eff},1/2}$ band and the ground state configuration of the system.

consistent with the atomic spacing of bulk Sr_2IrO_4 discussed above [see Fig. 1(b)]. A two-dimensional fast Fourier transform is presented in the inset of Fig. 2, where the positions of the four Bragg peaks are in agreement with the square grid of atoms as well.

Tunneling spectra were obtained by modulating the sample bias voltage and measuring the differential tunneling conductance with a lock-in amplifier at 77 K (Fig. 3) and 4.2 K (Fig. 4). For spectroscopy, we used an intentionally blunt gold tip to spatially average the measurement [21]. The high-temperature tunneling spectra (77 K) displayed as a solid red curve in Fig. 3 have a small density of states at the Fermi energy ($V_{\text{bias}} = 0$). The spectra have rough symmetry between positive and negative energy. Away from the Fermi energy, the density of states rises and has a pair of prominent peaks indicated by solid triangles. The Mott gap was estimated from the dI/dV spectra at 77 K to be $2\Delta = 615$ meV and was determined from the fits (dashed line) which will be discussed in Sec. III.

Inside the charge gap additional shoulders, indicated by hollow triangles, are present. Since there is rough particle-hole symmetry and we did not observe any dependence on position, these features are unlikely to be caused by impurities. We interpret these shoulders as an inelastic loss feature due to a single magnon. Since the particle-hole asymmetry is attributed to the charge gap, we define the function g as the

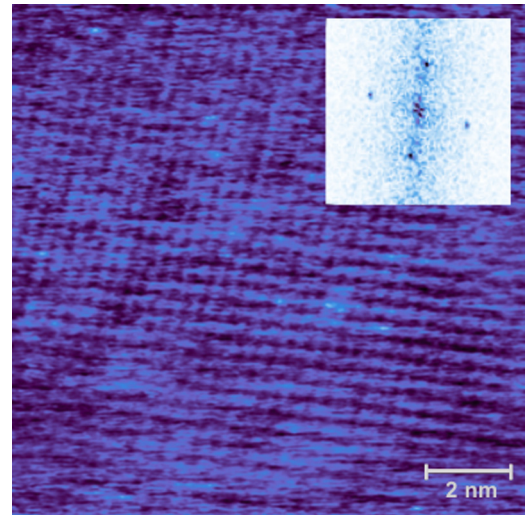


FIG. 2. (Color online) A high-resolution atomic-resolution topographic image of 12.2×12.2 nm² area of surface of Sr_2IrO_4 obtained with a constant current of $I_{\text{set}} = 600$ pA and $V_{\text{bias}} = 450$ mV. (Inset) Fast Fourier transform of topographic image.

even component of the dI/dV spectra [5]. Thus, the energy associated with this magnon is 105 meV as estimated from the peak position of the dg/dV spectra (blue) shown in the inset of Fig. 3. This value is in good agreement with the one from the calculated magnon density of states of Sr_2IrO_4 (light gray).

The low temperature tunneling spectra (4.2 K) are shown in Fig. 4. The density of states is clearly suppressed at the Fermi energy and rises away from zero bias. Both the Mott gap and single magnon (not shown) were also observed at low temperature with no obvious temperature dependence in this range. For small voltage bias ($|V_{\text{bias}}| < 50$ meV), additional slightly asymmetric features which are completely suppressed at high temperature appear. In an analysis similar to before the derivative of the function (g) was extracted from the STS and is presented in the inset of Fig. 4. Bulk magnetometry and muon spin relaxation show changes in magnetic order at

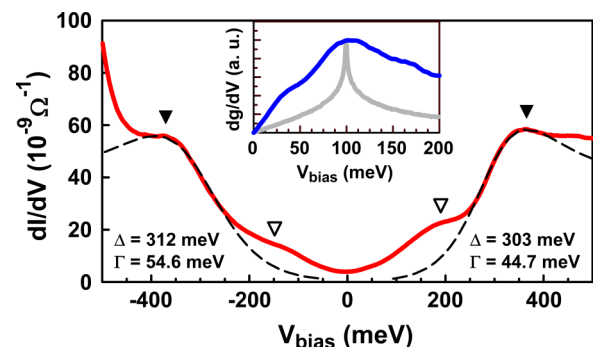


FIG. 3. (Color online) Scanning tunneling spectroscopy (solid red) of Sr_2IrO_4 at 77 K with modulation voltage 4 mV and frequency 703.4 Hz. The energy gap Δ and width Γ of the density of states from fits to Eq. (2) (dashed line) are displayed. (Inset) Inelastic electron tunneling spectroscopy (blue) and magnon density of states (light gray). The magnon dispersion has exchange energies $J_1 = 60$ meV, $J_2 = -20$ meV, and $J_3 = 15$ meV (Ref. [4]).

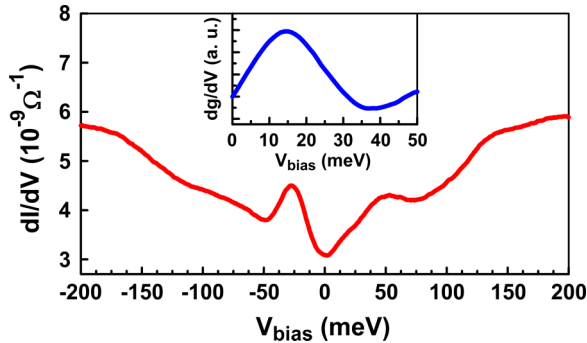


FIG. 4. (Color online) Scanning tunneling spectroscopy (red) of Sr₂IrO₄ at 4.2 K with modulation voltage 10 mV and frequency 704.2 Hz. (Inset) Inelastic electron tunneling spectroscopy (blue).

roughly 25 and 100 K [17]. We interpret the peak at ~ 15 meV (Fig. 4 inset) to be related to the magnetic ordering below 25 K [22].

III. ANALYSIS

The broad peaks in the high temperature differential tunneling conductance in Fig. 3 were fitted (dashed line, separate fits to peaks above and below Fermi energy) using the standard tunneling formalism [23] and the density of states of the half-filled, one-band Hubbard model on a square lattice [16]:

$$H = -t \sum_{\langle i,j \rangle, \sigma} (c_{i,\sigma}^\dagger c_{j,\sigma} + \text{H.c.}) + U \sum_{i=1}^N n_{i,\uparrow} n_{i,\downarrow}, \quad (1)$$

where t , $c_{i,\sigma}^\dagger$ ($c_{i,\sigma}$), and $n_{i,\sigma}$ are the hopping integral, creation (annihilation) operator, and number operator, respectively, for electrons at atomic site i with spin σ . Within the Slater mean-field approximation, the differential tunneling spectra can be expressed as [24]

$$\frac{dI}{dV} \propto \int_{-\infty}^{\infty} dE \frac{|E|}{\sqrt{E^2 - \Delta^2}} \frac{e^{(E+eV)/\Gamma}}{\Gamma(1 + e^{(E+eV)/\Gamma})^2}, \quad (2)$$

where Γ and Δ are treated as fit parameters.

From the fits to the STS, we infer the size of the insulating gap to be $2\Delta = 615$ meV. In addition, we were able to estimate the magnitude of the single-particle gap parameter, within the Slater approximation, to be $2\Delta = \frac{4}{3}U|\vec{S}_0| \approx 800$ meV, where $U \approx 2.0$ eV and $|\vec{S}_0| = 0.307$ are, respectively, the on-site Coulomb interaction and staggered magnetic moment [16,24]. Although the size of the gap measured through tunneling spectroscopy is smaller than expected within the Slater approximation, it is consistent with the ARPES result, $2\Delta \approx 560$ meV [2]. Also, the results from both RIXS [4] and

optical spectroscopy [3] are roughly 400 meV, which is smaller than the value we measured in this study.

Likewise, we infer the broadening parameter (Γ) to be 44.7 meV (54.6 meV) from fitting the peak at positive (negative) bias which is much larger than expected. As a result the width of this gap feature at 77 K is not solely due to thermal excitations. We interpret this broadening as evidence of electron-electron correlation, which is not captured by the Slater mean-field approximation. Conversely, the peak in the density of states is narrower than expected from results obtained within the dynamical mean-field approximation to the one-band, half-filled Hubbard model on the square lattice [25]. Thus neither the Slater nor dynamical mean-field approximations fully describes the underlying physics of Sr₂IrO₄.

As discussed above, shoulders are observed inside the Mott gap which we interpret as a single magnon. Its magnitude is estimated from the peak position of the tunneling spectra (blue) shown in the inset of Fig. 3 to be 105 meV. We were able to determine the magnon density of states (light gray) by summing the energy dispersion over the Brillouin zone [26]. The good agreement between the peak position of this calculation and our experimental results strongly support this single magnon interpretation. In addition, from RIXS measurements the magnon dispersion flattens around 120 meV creating a large increase in the density of states [4]. Similarly, the two magnon determined from Raman spectroscopy [8] is 240 meV and infrared spectroscopy [9] is 232 meV, which are roughly twice the value of the single magnon in Fig. 3, and are thus consistent with the results in this study.

IV. CONCLUSIONS

We have examined the properties of Sr₂IrO₄ with an STM. We were able to acquire atomically-resolved topographic images of the sample surface. We have measured the Mott gap of this material with tunneling spectroscopy to be $2\Delta = 615$ meV at 77 K, which is comparable to similar results from ARPES, RIXS, and optical conductivity measurements. We have modeled our results with the single-band Hubbard model and the Slater mean-field approximation. In addition, we saw a single-magnon excitation at an energy of 105 meV, which is consistent with magnons measured through other techniques. Also, we have observed a low-energy feature at roughly 15 meV that manifests itself at lower temperatures, which is likely due to additional magnetic ordering.

ACKNOWLEDGMENTS

This research was supported by NSF Grant Nos. DMR-0800367, DMR-0856234, and EPS-0814194. N.B.-A. acknowledges support from the National Research Council Postdoctoral Research Associateship Program.

[1] S. Chikara, O. Korneta, W. P. Crummett, L. E. DeLong, P. Schlottmann, and G. Cao, *Phys. Rev. B* **80**, 140407 (2009).

[2] Q. Wang, Y. Cao, J. A. Waugh, S. R. Park, T. F. Qi, O. B. Korneta, G. Cao, and D. S. Dessau, *Phys. Rev. B* **87**, 245109 (2013).

- [3] S. J. Moon, H. Jin, W. S. Choi, J. S. Lee, S. S. A. Seo, J. Yu, G. Cao, T. W. Noh, and Y. S. Lee, *Phys. Rev. B* **80**, 195110 (2009).
- [4] J. Kim, D. Casa, M. H. Upton, T. Gog, Y.-J. Kim, J. F. Mitchell, M. van Veenendaal, M. Daghofer, J. van den Brink, G. Khaliullin, and B. J. Kim, *Phys. Rev. Lett.* **108**, 177003 (2012).
- [5] D. C. Tsui, R. E. Dietz, and L. R. Walker, *Phys. Rev. Lett.* **27**, 1729 (1971).
- [6] J. Kua, L. J. Lauhon, W. Ho, and W. A. Goddard III, *J. Chem. Phys.* **115**, 5620 (2001).
- [7] A. J. Heinrich, J. A. Gupta, C. P. Lutz, and D. M. Eigler, *Science* **306**, 5695 (2004).
- [8] M. F. Cetin, P. Lemmens, V. Gnezdilov, D. Wulferding, D. Menzel, T. Takayama, K. Ohashi, and H. Takagi, *Phys. Rev. B* **85**, 195148 (2012).
- [9] Y. Hirata, H. Tajima, and K. Ohgushi, *J. Phys. Soc. Jpn.* **82**, 035002 (2013).
- [10] J. Dai, E. Calleja, G. Cao, and K. McElroy, *arXiv:1303.3688*.
- [11] Q. Li, G. Cao, S. Okamoto, J. Yi, W. Lin, B. C. Sales, J. Yan, R. Arita, J. Kuneš, A. V. Kozhevnikov, A. G. Eguiluz, M. Imada, Z. Gai, M. Pan, and D. G. Mandrus, *Sci. Rep.* **3**, 3073 (2013).
- [12] M. K. Crawford, M. A. Subramanian, R. L. Harlow, J. A. Fernandez-Baca, Z. R. Wang, and D. C. Johnston, *Phys. Rev. B* **49**, 9198 (1994).
- [13] B. J. Kim, H. Jin, S. J. Moon, J.-Y. Kim, B.-G. Park, C. S. Leem, J. Yu, T. W. Noh, C. Kim, S.-J. Oh, J.-H. Park, V. Durairaj, G. Cao, and E. Rotenberg, *Phys. Rev. Lett.* **101**, 076402 (2008).
- [14] B. J. Kim, H. Ohsumi, T. Komesu, S. Sakai, T. Morita, H. Takagi, and T. Arima, *Science* **323**, 1329 (2009).
- [15] G. Cao, J. Bolivar, S. McCall, J. E. Crow, and R. P. Guertin, *Phys. Rev. B* **57**, R11039 (1998).
- [16] F. Wang and T. Senthil, *Phys. Rev. Lett.* **106**, 136402 (2011).
- [17] M. Ge, T. F. Qi, O. B. Korneta, D. E. De Long, P. Schlottmann, W. P. Crummett, and G. Cao, *Phys. Rev. B* **84**, 100402 (2011).
- [18] A. Bautista, V. Durairaj, S. Chikara, G. Cao, K.-W. Ng, and A. Gupta, *Solid State Commun.* **148**, 240 (2008).
- [19] C. Ye, P. Cai, R. Yu, X. Zhou, W. Ruan, Q. Liu, C. Jin, and Y. Wang, *Nat. Commun.* **4**, 1365 (2013).
- [20] S. H. Pan, E. W. Hudson, and J. C. Davis, *Rev. Sci. Instrum.* **70**, 1459 (1999).
- [21] T. Kwapiński and M. Jałochowski, *Surf. Sci.* **604**, 1752 (2010).
- [22] In addition, the transition at 100 K is likely responsible for the shoulder at roughly 40 meV in the inset of Fig. 3.
- [23] M. Tinkham, *Introduction to Superconductivity* (McGraw Hill, Inc., New York, 1996), 2nd ed.
- [24] E. Fradkin, *Field Theories of Condensed Matter Systems* (Addison-Wesley Publishing, Redwood City, CA, 1991).
- [25] X. Wang, E. Gull, L. de' Medici, M. Capone, and A. J. Millis, *Phys. Rev. B* **80**, 045101 (2009).
- [26] From Eqs. (29) and (30) in the Supplemental Material of Ref. 4.